Endocytosis and Intracellular Fate of Liposomes Using Pyranine as a Probe†

Robert M. Straubinger,*,‡ Demetrios Papahadjopoulos,*,§,∥ and Keelung Hong*,∥

Department of Pharmacology and Cancer Research Institute, University of California, San Francisco, California 94143, and Department of Pharmaceutics, University at Buffalo, State University of New York, Amherst, New York 14260

Received October 16, 1989; Revised Manuscript Received January 8, 1990

ABSTRACT: Lipid vesicles (liposomes) containing pH-sensitive fluorophores were used as probes for the study of liposome entry and intracellular fate. Pyranine [8-hydroxy-1,3,6-pyrenetrisulfonate (HPTS)] was entrapped in the liposome aqueous core during preparation to provide a means of detecting internalization into living cells. HPTS is highly water soluble and shows a strong pH-dependent shift in its fluorescence excitation spectrum. Fluorescence emission (F_{EM}) is slightly pH dependent with excitation (λ_{EX}) at 350–415 nm but highly pH dependent with λ_{EX} at 450 nm. Liposomes bearing a net negative charge bound rapidly to CV-1 cells and underwent endocytosis. One hour after liposome addition, high F_{EM} with λ_{EX} at 413 nm and low F_{EM} with λ_{EX} at 450 nm suggest that most cell-associated liposomes had been internalized and resided at a mean pH of ~6.6. Collapse of cellular H^+ gradients with NH_4Cl or monensin treatment rapidly and reversibly increased F_{EM} with λ_{EX} at 450 nm. Direct examination by fluorescence microscopy corroborates the fluorometric data on internalization; over time, F_{EM} remained high with λ_{EX} at 350–405 nm but decreased with λ_{EX} at 450–490 nm, showing that all lipid vesicles were internalized within 40 min at 37 °C. Acidification of intracellular liposomes increased over 3 h, reaching a minimum value of approximately pH 5.5. HPTS persisted within acidic cellular vesicles for 2–3 days, and cytoplasmic dye was observed infrequently, suggesting that liposome fusion with cellular membranes seldom occurs. Material delivered to the endocytic pathway via lipid vesicles labeled an assortment of intracellular organelles of varying motility and morphology, including dynamic tubular structures whose lumen is acidic.

Liposomes have been used as model systems to study the biochemistry and biophysics of membrane processes, as probes of cellular function, and as carriers for cellular delivery of biologically active agents in vivo and in vitro. As model systems, they have contributed to the substantial progress made toward understanding membrane aspects of cellular (Hong et al., 1987; Meers et al., 1987) and viral fusion (White et al., 1980, 1982; Klappe et al., 1986; Nir et al., 1986), and the functional role of clathrin-associated components in receptor-mediated endocytosis (Chin et al., 1989). With regard to applications as carriers of macromolecules, liposomes containing chemotherapeutic agents are under evaluation for use against a variety of parasitic, fungal, and neoplastic diseases of humans (Mayhew & Papahadjopoulos, 1983; Mayhew et al., 1984; Lopez-Berestein et al., 1985). In vitro, liposomes have been used for cytoplasmic delivery of labile or membrane-impermeant compounds in order to modify cell behavior (Wilson et al., 1979; Fraley et al., 1981; Reisine et al., 1986; Connor & Huang, 1986).

Further development of liposomes for cell-biological and medical applications requires a detailed understanding of the mechanisms by which they interact with cells. Perhaps because of certain unique properties of liposomes, some early investigations of liposome–cell interaction concluded that fusion of liposomes with the plasma membrane occurred with high frequency. Recent evidence suggests that liposomes composed of charged phospholipids or ligand-directed by means of surface-linked immunoglobulins may be endocytosed by cells (Machy et al., 1982; Heath et al., 1983; Huang et al., 1983; Straubinger et al., 1983; Truneh et al., 1983). Liposomes can enter cells through the coated pit/coated vesicle system (Straubinger et al., 1983) that is associated with internalization of many viruses or nutritional and signal molecules (Brown & Goldstein, 1979; Brown et al., 1983; Steinman et al., 1983; Mellman et al., 1986). It is not known currently how such encapsulated macromolecules as RNA (Wilson et al., 1979), DNA (Fraley et al., 1981), proteins (Gardas & Macpherson, 1979; McIntosh & Heath, 1982), or highly charged small molecules (Heath et al., 1983) escape the endocytic pathway and gain access to the cytoplasm functionally intact.

In order to study the intracellular disposition of liposomes, our approach was to improve detection by light microscopy or fluorometry of the acidification of lipid vesicle aqueous contents (Hong et al., 1986), using hydroxypyrenetrisulfonate (HPTS),[1] as a fluorescence indicator for pH measurements in the physiological range. Fluorometry has been used to provide a quantitative assessment of liposome endocytosis by populations of cells, and fluorescence microscopy has been used to provide a qualitative view of the intra- and intercellular heterogeneity of liposome uptake.

Materials and Methods

Reagents. HPTS was purchased from Molecular Probes (Eugene, OR) and did not require subsequent repurification. A 35 mM solution was prepared in 10 mM HEPES buffer, pH 7.4; NaCl was added to adjust the osmolality to 300 mOs/kg. Phosphatidylserine (from bovine brain) and phos-

† This work was supported by Grants CA-35340 and CA-25526 from the National Institutes of Health.

* Address correspondence to either author.

‡ Department of Pharmaceutics, 539 Cooke Hall, University at Buffalo, SUNY. Electronic mail: rms@acsu.buffalo.bitnet (or .edu).

§ Department of Pharmacology, University of California.

∥ Cancer Research Institute, University of California.

[1] Abbreviations: CHOL, cholesterol; EDTA, ethylenediaminetetraacetate; F_{EM}, fluorescence emission intensity; HPTS, 8-hydroxy-1,3,6-pyrenetrisulfonate; PBS, Dulbecco's phosphate-buffered saline; PBS/CM, PBS with 0.4 mM Ca^{2+} and 0.4 mM Mg^{2+}; PC, phosphatidylcholine; PS, phosphatidylserine; λ_{EX}, fluorescence excitation wavelength.

0006-2960/90/0429-4929$02.50/0

phatidylcholine (from egg yolk) were purchased from Avanti Polar Lipids (Birmingham, AL). Cholesterol was obtained from Sigma (St. Louis, MO) and was recrystallized three times from methanol. Lipids were stored in sealed ampules under argon at −70 °C.

Liposome Preparation. HPTS-containing liposomes were prepared by the reverse-phase evaporation (REV) procedure (Szoka & Papahadjopoulos, 1978) and were extruded through polycarbonate filters (pore diameter, 0.1 μm) to define their final diameter (Szoka et al., 1980). Unencapsulated HPTS was removed by chromatography on a Sephadex G-75 column (1 × 15 cm) equilibrated with 150 mM NaCl and 5 mM HEPES, pH 7.4. Phospholipid concentration was determined by the method of Bartlett (1959).

Cell Culture and Liposome–Cell Incubation. CV-1, an established line of African green monkey kidney cells, was cultured in complete growth medium, consisting of Dulbecco's modified Eagle's medium (DMEM) supplemented with 3 g/L D-glucose and 5% bovine newborn serum. Cells grown on coverslips or in 66-mm plastic culture dishes (Falcon) were treated with HPTS liposomes as described in Straubinger et al. (1983). Unless stated otherwise, cells in growth medium were washed twice with PBS containing 0.36 mM Ca^{2+} and 0.42 mM Mg^{2+} (PBS/CM). HPTS liposomes were diluted with PBS/CM (supplemented with 5 mM glucose) to 500 μM phospholipid; 0.2 mL (0.1 μmol of phospholipid) was added to each dish of 10^6 cells. After 30 min in a humidified incubator at 37 °C, cells were washed twice with PBS/CM and analyzed for fluorescence. To examine liposome internalization at longer times, cells were returned to complete growth medium and incubated at 37 °C.

Fluorometric Analysis. Fluorescence was monitored with a SPEX Fluorolog 2 equipped with a photon-counting detector. The temperature of the sample was controlled at 20 °C with a circulating water bath. For determinations of HPTS spectra for cell suspensions, cells in PBS/glucose were mixed gently with a magnetic stirbar, and 5×10^5 cells/mL was used for each time point. For experiments in which cells grown on a glass coverslip were used for the fluorescence measurements, the coverslip was inserted diagonally into a cuvette and held in place by a thin Teflon holder. The monolayer of cells on the coverslip was oriented to minimize reflection from the coverslip. All fluorescence intensity measurements were taken in the ratio mode, with rhodamine used as a reference, to correct for wavelength-dependent variations in excitation beam intensity. Spectra were otherwise uncorrected. Background fluorescence typically amounted to 1% of the fluorescence signal and was not subtracted from the data.

Fluorescence Microscopy. Two standard filter cubes were used to define the excitation wavelengths for viewing HPTS fluorescence by microscopy. The pH-independent fluorescence of HPTS could be viewed with Leitz filter set B, which excites in a wide violet band (350–410 nm). Emission was defined with a long-wave-pass dichroic mirror (455 nm) and a long-pass barrier filter (445 nm). The second filter set (Leitz I2), having a narrow blue excitation band (450–490 nm), a long-pass dichroic mirror (510 nm), and a long-pass barrier filter (515 nm), was used to visualize exclusively the fluorescence of HPTS at neutral or basic pH. The violet filter set is commonly used for Hoechst DNA stains and the blue for fluorescein. Photographs of fluorescence and phase-contrast fields were made on Fuji color print film at ISO (ASA) 1600. Except where stated, the proper exposure was automatically determined by a field-averaging meter, so the relative fluorescence intensity of some fields cannot be determined from the figures. Prints for publication were made on Agfa TP6WP high-contrast paper, and where indicated, photographs from the same roll of film were printed under identical conditions to show comparative intensity differences.

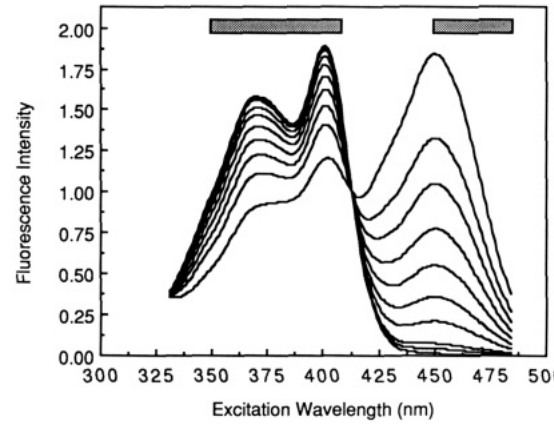

FIGURE 1: Excitation spectra of HPTS in the pH range 4.5–7.4. Seven micromolar HPTS in PBS/CM was adjusted to various pHs, and the excitation wavelength (λ_{EX}) was scanned over the range 330–480 nm. Fluorescence emission (F_{EM}) was detected at 510 nm. The curves represent pH 7.4, 7.1, 6.9, 6.7, 6.5, 6.3, 6.0, 5.5, 5.25, and 4.5. The pH 7.5 curve can be identified as that with the highest intensity at 450 nm and the lowest intensity at 350–400 nm. The isosbestic wavelength is 413 nm. Stippled bars over the spectra indicate the excitation wavelength ranges for the filter sets used in fluorescence microscopy (cf. Figures 4–7 and 10).

Calibration curves for the pH dependence of HPTS fluorescence were constructed as follows. Seven micromolar HPTS in PBS/CM was adjusted to various pHs and placed in a chamber slide having a focusing target. The slide was mounted on the microscope, equipped with a 100-W Hg lamp and Nikon automatic exposure system that has a digital readout for seconds of exposure. Exposure time calculated by the camera photometer is linear with respect to light intensity and was recorded for both the wide-band violet ($\lambda_{EX\ VIOLET}$) and narrow-band blue ($\lambda_{EX\ BLUE}$) filter systems. Four determinations were made at each pH, and repetitive determinations were made on different days. pH of the dye solutions was verified during each calibration.

Video fluorescence microscopy was performed as described above but with several modifications. The light source was a variable-intensity halogen lamp, which allowed low illumination of samples. Video images were made with a Cohu silicon-intensifier (ISIT) video camera and recorded on video tape. Frames for publication were photographed subsequently from a video monitor.

RESULTS

pH-Dependent Spectral Properties of HPTS. HPTS (8-hydroxy-1,3,6-pyrenetrisulfonate) is a water-soluble compound of high quantum yield, whose absorption spectrum is markedly pH dependent. The pH dependence of HPTS fluorescence intensity is the result of reversible proton dissociation from a lone hydroxyl group on the trisulfonated pyrene ring. Fluorescence (F_{EM}) increases with pH when excitation is at (λ_{EX}) 450 nm and decreases when excitation is at 350–405 nm (Figure 1). Fluorescence intensity is pH independent at λ_{EX} 413 nm, the isosbestic wavelength of the excitation spectrum. HPTS is a suitable marker for use in fluorescence microscopy because substitution of the pyrene ring shifts the fluorescence spectrum into a range that is easily achieved with standard optics.

The pH-dependent spectral properties of HPTS did not change when the dye was encapsulated in negatively charged

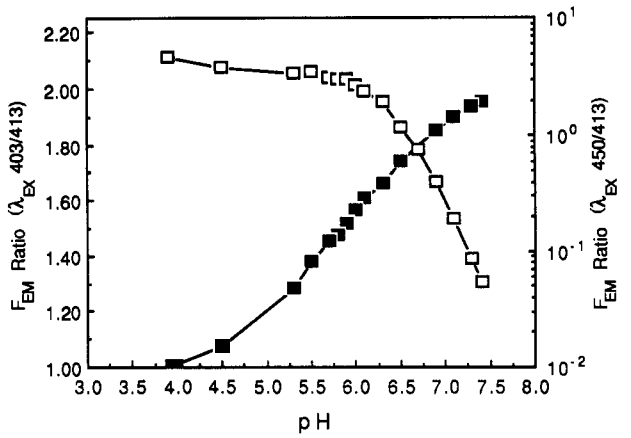

FIGURE 2: pH calibration curves for HPTS. Ratios were calculated for fluorescence emission intensity (F_{EM} 510 nm) as a function of pH, with λ_{EX} 450/413 nm (filled symbols) or λ_{EX} 403/413 nm (open symbols). The data, taken from Figure 1, allow conversion of ratios to approximate pH reported by HPTS.

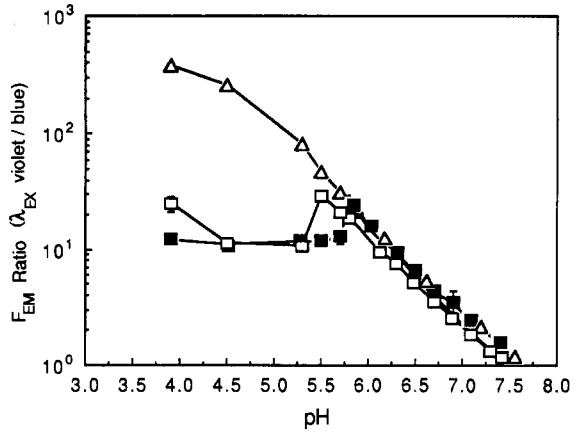

FIGURE 3: pH calibration curves for HPTS: fluorescence microscope determinations. Seven micromolar HPTS in PBS/CM was adjusted to various pHs and placed in a chamber slide. Fluorescence emission was measured for the two excitation/emission filter sets (violet band and blue band) used to observe HPTS-loaded cells. Measurements were performed as described under Materials and Methods. Each point represents the ratio of the mean emission intensity, and vertical bars represent one standard deviation. In most cases, plot symbols are larger than the standard deviation of the measurements. Data are plotted as the inverse with respect to Figure 2 because the photometer signal is inversely related to light intensity. (Open squares) Ratio of $\lambda_{EX\ VIOLET}/\lambda_{EX\ BLUE}$ for the 25× objective lens; (filled squares) ratio of $\lambda_{EX\ VIOLET}/\lambda_{EX\ BLUE}$ for the 63× objective lens. Triangle symbols show the theoretical response of the filter sets; values were calculated by numerical integration of appropriate regions (λ_{EX} 350–410 nm and λ_{EX} 450–490 nm) of the spectra in Figure 1.

liposomes composed of phosphatidylserine, phosphatidylcholine, and cholesterol (PS/PC/CHOL, 1:1:1 mole ratio). The emission maximum was 510 nm (not shown), with excitation maxima at 450 and 403 nm (Figure 1). The fluorescence intensity of encapsulated HPTS was invariant at the isosbestic wavelength (λ_{EX} 413 nm) and therefore is a measure of total cell-associated liposomes. pH can be determined by taking the ratio of F_{EM} with excitation at pH-dependent and pH-independent wavelengths.

The fluorescence spectra of HPTS (Figure 1) were used to construct a calibration curve of emission intensity ratios as a function of pH (Figure 2). F_{EM} ratios from both the λ_{EX} 450/413 nm and the λ_{EX} 403/413 nm pairs are useful in reporting physiological pH. With λ_{EX} 403/413, the F_{EM} ratio increases to a constant value (2.0) below pH 6.0. In contrast, the F_{EM} ratio with λ_{EX} 450/413 nm decreases with pH to a small value (0.05 at pH 5.0). In practice, many wavelength combinations in the pH-sensitive excitation bands from 350–405 and 410–470 nm may be used for calculation of pH, with appropriate background correction and calibration. For the studies here, the λ_{EX} 450/413 nm ratio proved highly sensitive, changing 2 orders of magnitude in the pH range of 4–7.4. By comparison, Ohkuma and Poole (1978) showed that fluorescein-based probes undergo less than a 9-fold change in the λ_{EX} 495/450 nm ratio over the same pH range.

Stability of Encapsulated HPTS and Liposome Permeability to H^+. HPTS is highly water soluble, even at acidic pH, where the phenolate group is protonated. However, previous work (Szoka et al., 1979; Straubinger et al., 1983; Barbet et al., 1984) showed that some aqueous dyes that are membrane impermeant at neutral pH become permeant under mildly acidic conditions. To measure the efflux of encapsulated dye, HPTS liposomes were dialyzed against isotonic buffers over a pH range from 4 to 7.4 for 48 h. Less than 1% of the total HPTS encapsulated in PS/PC/CHOL (1:1:1) liposomes was measured in the dialyzate (not shown). That value would be expected from previous experiments (Clement & Gould, 1981) with liposomes of a simpler composition and prepared by a different procedure, which also showed that phospholipid bilayers are impermeant to the highly charged HPTS.

The permeability of membranes to protons varies with a variety of factors. To investigate whether endocytosed liposomes would report the pH of their external environment with an acceptable time constant, we determined the rate of pH equilibration for the PS/PC/CHOL liposomes used in these studies. Liposomes in isotonic buffer were subjected to an abrupt change in pH, and F_{EM} was monitored at 510 nm. The excitation wavelength was 450 nm. When the pH was lowered from 7.4 to 4.5 by injection of small volumes of either acetic or citric acid, proton equilibration across the bilayer was rapid and virtually complete in 6 s at 20 °C (data not shown). Therefore, encapsulated HPTS should report the pH of the environment in which they reside, provided the buffering capacity of the dye is not large compared to the ability of endocytic vesicles to maintain a proton gradient.

Fluorescence Microscopy of Liposome Endocytosis: Calibration. Commonly used fluorescence microscope filter sets produce acceptable excitation bands for detecting pH-dependent changes in HPTS emission. A violet filter set (λ_{EX} 350–410 nm) used for such dyes as Hoechst DNA stains excites HPTS over a range of wavelengths for which F_{EM} increases slightly in response to acidification (Figure 1). Blue filter sets (λ_{EX} 450–490 nm) used for fluorescein excite HPTS in the most pH-sensitive region of its spectrum; acidification is manifested as a strong decrease in fluorescence emission. Figure 3 shows the theoretical response of the two microscope filter systems, obtained from the observed spectra in Figure 1 by numerical integration over the range appropriate for the filters. Those ranges are indicated by bars over the spectra in Figure 1. It can be seen that the fluorescence microscope should be highly sensitive to shifts in the excitation spectrum that accompany acidification of HPTS in the pH range of 7.4–4.5. Over that range, the calculated ratio changes more than 100-fold. To estimate the actual pH dependence of HPTS fluorescence detected by microscopy, solutions of HPTS at various pH were placed in a chamber slide (see Materials and Methods). The dye concentration was chosen to give a fluorescence intensity comparable to that observed in experiments with cells (below). Fluorescence intensity was quantified with a photometer for both violet (λ_{EX} 350–410 nm) and blue (λ_{EX} 450–490 nm) excitation filter sets. Figure 3 shows the observed ratios of F_{EM} intensity ($\lambda_{EX\ VIOLET}/\lambda_{EX\ BLUE}$) for the two filter systems, over the pH range of 4.0–7.4. Data

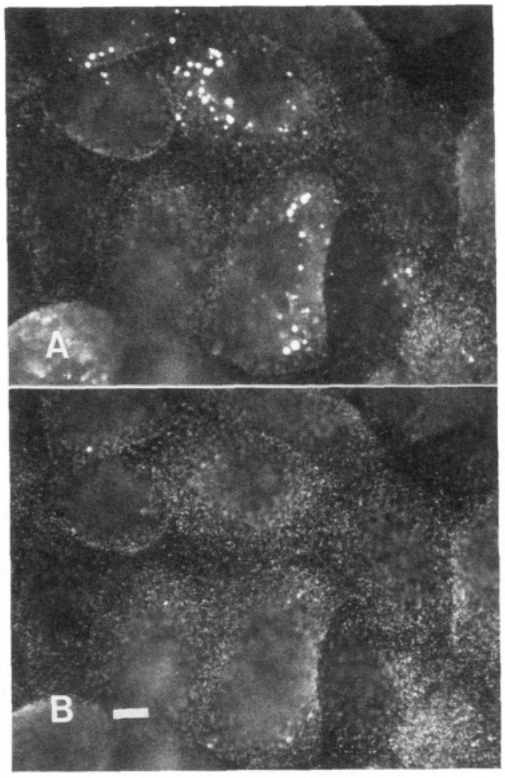

FIGURE 4: Endocytosis of HPTS-containing liposomes detected by differential fluorescence excitation. CV-1 cell monolayers on glass coverslips were exposed to 100 nmol of PS/PC/CHOL (1:1:1) liposomes containing 35 mM HPTS at 37 °C in PBS/CM glucose. At 15 min, cells were washed free of nonadherent liposomes and viewed under (A) violet (pH insensitive, $\lambda_{EX\ VIOLET}$) or (B) blue (pH sensitive, $\lambda_{EX\ BLUE}$) fluorescence excitation. Bars over the spectra in Figure 1 depict the wavelengths passed by the two filter sets. Violet excitation reveals total cell-associated dye, while blue shows that which resides in a compartment of approximately pH >6.5–6.8. Large, low-pH punctates visible only in (A) ($\lambda_{EX\ VIOLET}$) likely represent intracellular vesicles into which liposome-entrapped HPTS has leaked after endocytosis of liposomes. Bar: 10 μm.

are plotted as the inverse, relative to the ratios in Figure 2, to simplify calculation from the raw photometer data (photometer signal output is inversely proportional to light intensity).

Figure 3 shows that from pH 5.5 to pH 7.4 the F_{EM} ratio for $\lambda_{EX\ VIOLET}/\lambda_{EX\ BLUE}$ shows a pH dependence close to that predicted from spectral data and changes 20-fold in magnitude. Below pH 5.5, the observed ratio diverges from that calculated from excitation scans and reaches a plateau. pH-dependent quenching of the 450-nm excitation peak ($\lambda_{EX\ BLUE}$) ultimately results in fluorescence intensity below the sensitivity of the photometer. Although higher concentrations of HPTS extend the useful range of quantitation below pH 5.5 (data not shown), the concentration of dye used here represents an amount within the range found in experiments described below.

Endocytosis and Cellular Processing of HPTS-Containing Liposomes. CV-1 cells were grown to confluence on glass coverslips and washed free of growth medium. Cells were incubated with PS/PC/CHOL liposomes at 37 °C in glucose-containing buffer. Observation of cells by fluorescence microscopy 15 min after addition of HPTS liposomes showed substantial association of dye with cells. When viewed under violet illumination (Figure 4A), which irradiates HPTS in a region of its spectrum that is largely pH independent, liposomes were visible as punctate fluorescence sources. Both large- and small-diameter fluorescent localizations can be seen in Figure 4A. Viewed under blue illumination (Figure 4B), which excites HPTS in a highly pH-sensitive band, most small punctates remained visible, but some larger, intense localizations of fluorescence were not visible. HPTS liposomes visible with blue excitation likely were on the cell surface, but we cannot exclude the possibility they represent intracellular vesicles not acidified below pH 6.5–6.8. Under blue excitation, HPTS fluorescence at pH 6.5 is one-third that at pH 7.4 (Figure 1), a difference detected easily by the observer. However, the photometer configuration does not allow measurement of single punctates, so a more accurate estimate of vesicular pH cannot be made against a background of liposomes on the cell surface. HPTS visible under violet illumination, but not visible under blue, corresponds to dye in an acidic compartment. The apparently larger diameter of acidic punctates, visible in Figure 4A, may result from leakage of liposome contents into the surrounding vesicle lumen subsequent to endocytosis and delivery of dye to multivesicular bodies.

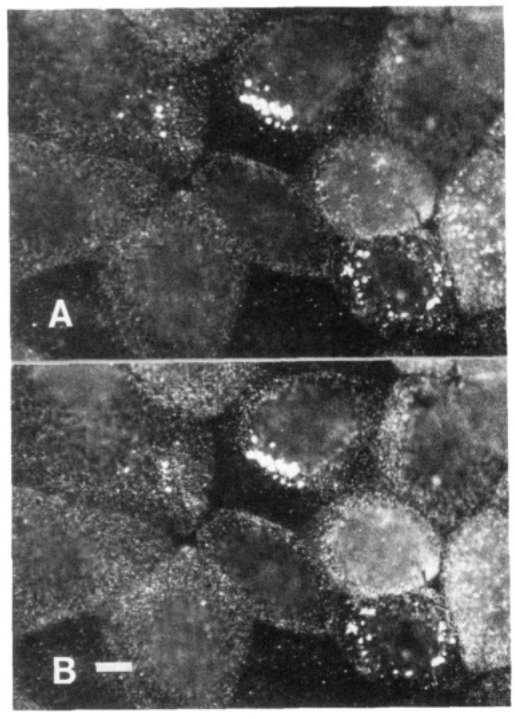

FIGURE 5: Effect of lysosomotropic agents on cell-associated HPTS. CV-1 cell monolayers were exposed to HPTS-containing liposomes for 15 min, as described in Figure 4. After fluorescent intensities were recorded under violet and blue excitation, 50 mM NH_4Cl was added to the cells, and the cells were photographed within 5 min. In contrast to Figure 4, virtually all punctates visible under the pH-dependent excitation (panel B, $\lambda_{EX\ BLUE}$) also are visible under the pH-independent excitation (panel A, $\lambda_{EX\ VIOLET}$), including large fluorescent vesicles having an appearance similar to that of the acidic vesicles shown in the absence of NH_4Cl (Figure 4). Bar: 10 μm.

To determine whether quenching of HPTS under blue excitation was the effect of an acidic environment, rather than a pH-independent effect such as degradation, cells were treated with lysosomotropic amines. Figure 5 shows cells treated for 15 min with HPTS liposomes as in Figure 4, washed, and then incubated in 50 mM NH_4Cl. Figure 5A shows total cell-associated HPTS (violet band illumination). Cells had fluorescent vesicles with morphology similar to that described above (Figure 4A). Within 2 min of exposure to NH_4Cl, fluorescent punctates not previously visible under blue illumination became apparent (Figure 5B). In contrast to Figure 4B, Figure 5B shows that all fluorescent punctates visible under (pH independent) violet excitation also were visible under (pH dependent) blue excitation in the presence of NH_4Cl. With removal of NH_4Cl, the effect was reversed within 2 min (data

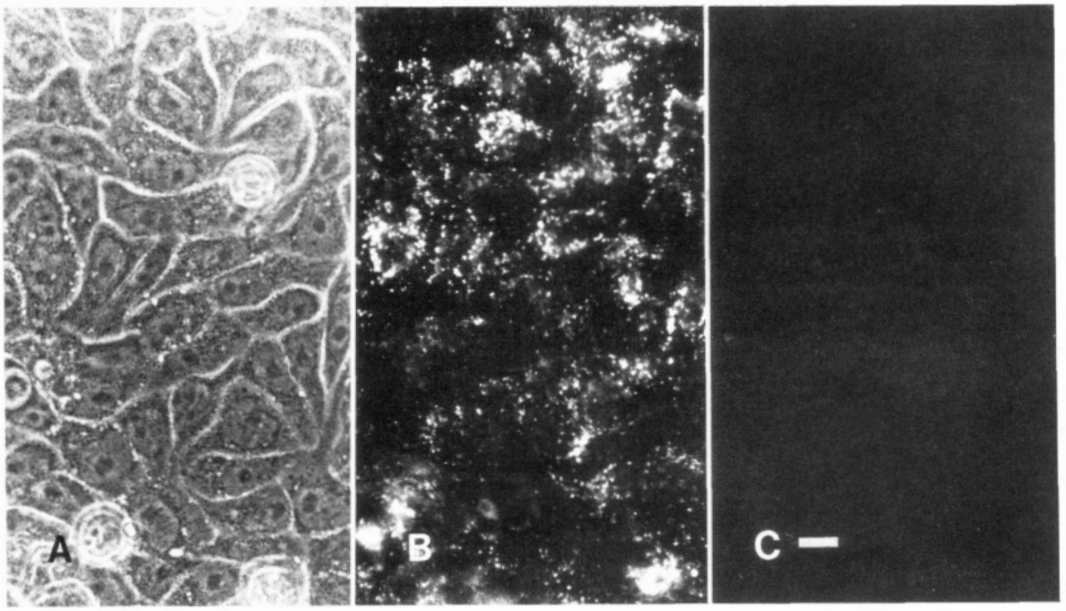

FIGURE 6: Increased acidification of cell-associated liposome contents with time. CV-1 cell monolayers were exposed to HPTS-containing liposomes for 30 min, as described in Figure 4, and then returned to complete growth medium for an additional 1.5 h before observation. (A) Phase-contrast image of CV-1 cell monolayer; (B) total cell-associated HPTS ($\lambda_{EX\ VIOLET}$); (C) neutral-pH HPTS fluorescence ($\lambda_{EX\ BLUE}$). The photographic exposure time in (B) was 9 s and in (C) was 64 s, giving a F_{EM} ratio for $\lambda_{EX\ VIOLET}/\lambda_{EX\ BLUE}$ of 7.1. Photographic conditions for the fields in (B) and (C) were identical with those used for panels A and B of Figure 4, respectively, in order to show relative intensity differences for short and long incubation times with liposomes. Bar: 10 μm.

not shown). Such results support the conclusions that HPTS not visible under blue illumination (λ_{EX} 450–490 nm) resided in intracellular vesicles of low pH.

To determine the longer term disposition of liposome-delivered HPTS, cells were incubated with HPTS-containing liposomes for 30 min and then returned to complete growth medium; 1.5 h after removal of unbound liposomes, virtually all cell-associated dye reported acidic pH. Figure 6C shows that little dye was detected under blue excitation. In contrast, cells were intensely fluorescent when viewed under violet illumination (Figure 6B). The photographic exposure times for fields in Figure 6 (panels B and C) were identical with those used in Figure 4 (panels A and B, respectively). Hence, the differences in intensity shown here reflect the differences observed in the microscope. The F_{EM} ratio was calculated from photometer data; the ratio reported for $\lambda_{EX\ VIOLET}/\lambda_{EX\ BLUE}$ was 7.1. From the data in Figure 3, that ratio corresponds to an approximate pH of 6.4. Given the high fraction of liposome-derived HPTS reporting an acidic environment, we infer nearly complete endocytosis of cell-associated liposomes within 1.5 h.

The distribution of fluorescence in many cells was nonuniform at 1.5 h and often concentrated in the perinuclear region (Figure 6B). Occasionally, patches of cells were observed that showed nonacidified liposomes (not shown). Thus the mean pH indicated by fluorometric measurements on populations of cells (described below) may underestimate endocytosis at 1.5 h.

By 3.0 h after removal of unbound liposomes, virtually no HPTS was detected with $\lambda_{EX\ BLUE}$, i.e., in nonacidic compartments. With $\lambda_{EX\ VIOLET}$, HPTS was observed in acidic perinuclear vesicles as well as in acidic, highly motile vesicles in the cell periphery (not shown, but similar to Figure 6). In addition, ramifying strands of an acidic tubular compartment also could be observed (not shown). Incubation of cells in NH_4Cl rapidly and reversibly revealed intracellular HPTS under $\lambda_{EX\ BLUE}$ (not shown).

Pinocytosis of Free HPTS. Significant efflux of liposome contents into the external medium occurred upon interaction with cells (10–15%; described below). Therefore, control experiments were performed with free HPTS to assess the contribution of pinocytic uptake of leaked dye to the results described for liposome endocytosis. Cells were exposed for 30 min to 35 μM free dye, equivalent to the concentration added to cells in liposomes, or to 350 μM dye, a 10-fold excess. pinocytic uptake of 35 μM HPTS was low, and fluorescence at any λ_{EX} was below the threshold of the microscope photometer (not shown). HPTS at 350 μM resulted in detectable labeling of intracellular vesicles. Cell-associated fluorescence was highly localized in a punctate pattern, and dye adsorption to the plasma membrane or diffusion into the cytoplasm was undetectable. Figure 7B shows total cell-associated HPTS under violet band illumination. Examination at the pH-sensitive wavelengths ($\lambda_{EX\ BLUE}$) showed that all cell-associated dye reported acidic pH (not shown), similar to the image shown above for liposome-delivered HPTS at 120 min (Figure 6C). Labeling of intracellular vesicles visible under phase-contrast illumination was neither uniform nor complete, suggesting temporal or physical compartmentalization of newly pinocytosed HPTS.

Kinetic Analysis of Liposome–Cell Association and Internalization. CV-1 cells on glass coverslips were incubated at 37 °C with 100 nmol of PS/PC/CHOL as described for fluorescence microscopy. After 15 or 30 min of incubation, cells were washed extensively in PBS/CM to remove free liposomes. Coverslips were either analyzed immediately in the fluorometer or incubated in complete growth medium for longer periods. Analysis consisted of repetitive scans over the range of excitation wavelengths from 370 to 470 nm. Full λ_{EX} spectra were taken to ensure that artifacts from autofluorescence, dye binding to cellular proteins, dye metabolism, or light scattering could be detected readily. Emission spectra at λ_{EX} 403, 413, and 450 nm were checked routinely under various conditions to verify that the emission peak did not shift from 510 nm.

After 15 min at 37 °C, liposome association with CV-1 cells was detectable, as determined by monitoring fluorescence with λ_{EX} 413 nm (Figure 8A), the pH-insensitive wavelength for

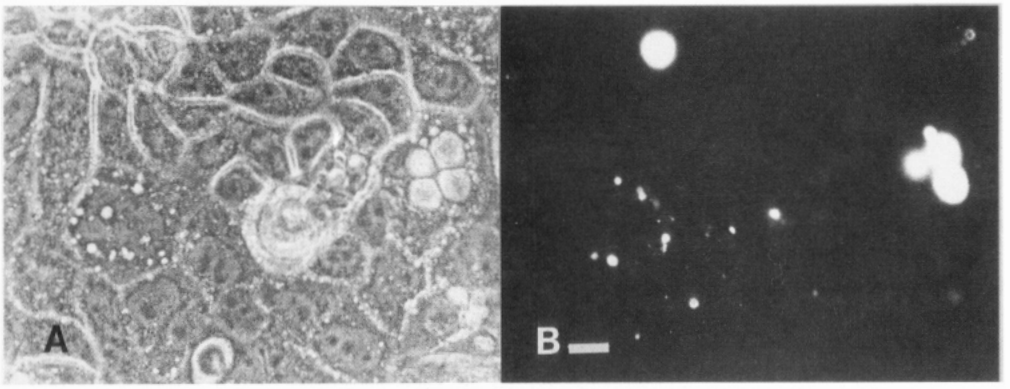

FIGURE 7: Pinocytosis of free HPTS by CV-1 cells. Cell monolayers were exposed for 30 min to concentrations of free HPTS 10-fold higher (350 μM) than those present in liposome experiments. (A) Phase-contrast image of CV-1 cell monolayer; (B) total cell-associated HPTS ($\lambda_{EX\ VIOLET}$). Not shown: neutral-pH HPTS fluorescence ($\lambda_{EX\ BLUE}$), since the field was similar to the dim field shown in Figure 6C. Bar: 10 μm.

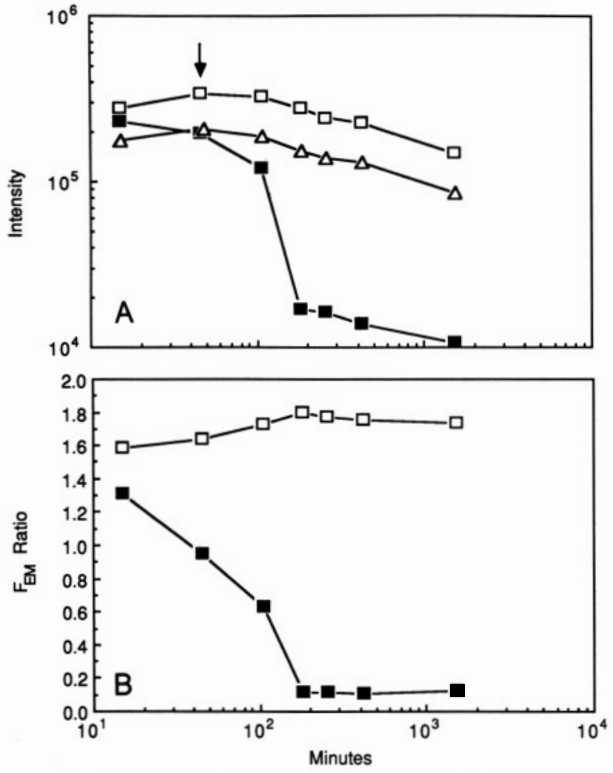

FIGURE 8: Endocytosis of HPTS liposomes: determinations from CV-1 cells on coverslips. CV-1 cell monolayers were exposed for 15 or 30 min to HPTS-containing liposomes as described in Figure 4. Coverslips were washed rapidly with 20 °C PBS/CM and placed in a cuvette containing the same buffer. For later time points, coverslips from cells exposed to liposomes for 30 min were placed in prewarmed, complete growth medium and incubated until the time indicated. Fluorescence analyses were completed in 45 s, and repetitive scans agreed closely. upper panel: fluorescence intensity (F_{EM}) at specific excitation wavelengths (λ_{EX}) as a function of time since liposome addition. F_{EM} was detected at 510 ± 4 nm. Excitation wavelengths were 403 (open squares), 413 (triangles), and 450 nm (filled squares). Lower panel: F_{EM} ratios for the three λ_{EX} shown in the upper panel. (Open symbols) 403/413 ratio; (filled symbols) 450/413 ratio.

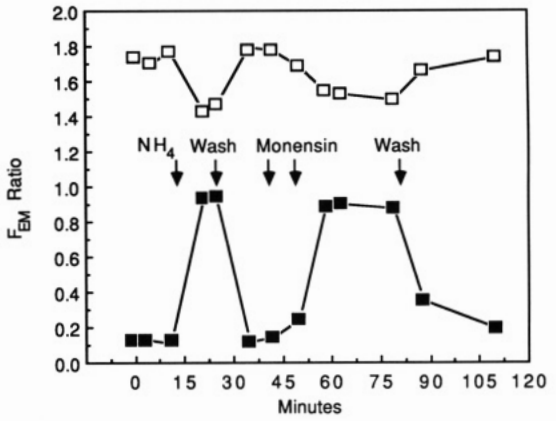

FIGURE 9: Effect of NH_4Cl and monensin on HPTS-loaded cells. CV-1 cells on coverslips were exposed to HPTS-containing liposomes of PS/PC/CHOL as in Figure 4 but were allowed to grow for 26 h before the fluorometric analysis described in Figure 8 was performed. Cells were washed free of growth medium and mounted in a cuvette in PBS/CM/glucose at 20 °C. At the times indicated, 50 mM NH_4Cl was added to the cuvette and then washed out. Subsequently, 15 μM monensin was added, followed by 100 μM monensin. As indicated, monensin was washed out.

HPTS. Cells continued to accumulate liposomes over an additional 15 min. At 30 min, exposure to liposomes was terminated by washing. Approximately 12–17% of liposomes added remained with cells, as determined by experiments with liposomes containing [^{14}C]sucrose (not shown). By determining the concentration of free and liposome-encapsulated HPTS in cell supernatants at 30 min and 1 h, we observed that PS/PC/CHOL (1:1:1) liposomes leak an increasing fraction of their contents with decreasing lipid concentration (Straubinger et al., 1988). At the concentrations used in the present work, approximately 12–15% of the contents are released into the medium; a 10-fold lower liposome concentration results in a doubling of the leakage rate (not shown). We infer that leakage may be mediated by a saturable cellular process of low capacity. It is unclear whether leakage results from liposome membrane disruption induced by cellular components or from rapid endocytosis and regurgitation upon recycling to the cell surface [cf. Haylett and Thilo (1986) and Goldmacher et al. (1986)].

Removal of free liposomes resulted in reduction of total cell-associated dye with time, as indicated by a decline in fluorescence intensity with λ_{EX} 413 nm (Figure 8A). From the data in Figure 8A, the reduction in cell-associated dye apparently is biphasic (analysis not shown); more than 30% of the HPTS fluorescence associated with cells at 30 min was lost over 4–5 h. An additional 30% reduction in F_{EM} occurred over the subsequent 20 h. Reduction may indicate shedding or leakage of liposomes or intracellular metabolism of HPTS (see below and Figure 9).

For all time points from 15 min to 3 h, we also observed a progressive reduction in fluorescence emission with λ_{EX} 450 (Figure 8A), consistent with the expected change due to acidification of HPTS. Over the same period, F_{EM} with λ_{EX} 403 also decreased, nearly in parallel with the decline in total cell-associated HPTS (shown by λ_{EX} 413 nm). Figure 8B

shows that the F_{EM} ratio with λ_{EX} 403/413 increased, consistent with acidification of HPTS. More dramatic changes over time were observed in the F_{EM} ratio with λ_{EX} 450/413, which decreased more than 10-fold over 3 h. Spectral changes indicated by both ratios are consistent with liposome internalization into a low-pH compartment.

The calibration curve in Figure 2 allows estimation of the mean pH reported for the liposome population (Figure 8B). Fifteen minutes after exposure to liposomes, the reported pH was 0.3 pH unit below that of the bulk external medium, or approximately pH 7.1. The value likely represents an underestimate of the amount of endocytosis, as liposomes reside both on the cell surface and in the endocytic pathway (cf. Figure 4). At 30 min, the mean pH reported by cell-associated HPTS was approximately 6.8. At 2 h (1.5 h after removal of free liposomes), the mean pH was 6.4, in excellent agreement with the value given by the fluorescence microscope photometer for fields of cells observed at the same time point (Figure 6). Over the subsequent hour, the pH fell to a maximal acidity of about 5.6, which was maintained for more than 24 h. Fluorescence microscopy revealed that few cells had surface liposomes at 1.5–2 h (Figure 6C), so the continuing fall in the reported pH may represent a progression of liposome contents to compartments of increasing acidity, subsequent to endocytosis of the surface pool of liposomes. Alternatively, dye in higher pH compartments may be regurgitated rather than acidified.

At 24 h, F_{EM} ratios for λ_{EX} 403/413 nm and λ_{EX} 450/413 nm were nearly unchanged from those of 3 h and corresponded to a maximal acidification of approximately pH 5.6. To determine whether the ratios represent HPTS in an acidic environment or pH-independent effects on the dye resulting from prolonged residence in the endocytic pathway, HPTS-loaded cells on coverslips were treated with NH_4Cl or monensin. The former is a lysosomotropic amine (DeDuve et al., 1974), and the latter is a H^+ ionophore [reviewed in Tartakoff (1983)]; both have the effect of raising the lumen pH of acidic intracellular organelles [Maxfield, 1982; reviewed in Brown et al. (1983) and Mellman et al. (1986)]. Figure 9 shows that NH_4Cl rapidly and reversibly changed the F_{EM} ratio for both λ_{EX} 403/413 nm and λ_{EX} 450/413 nm, in a manner consistent with alkalinization of the compartment in which HPTS resided. Alkalinization was nearly maximal within 1.5–2 min of addition, and we calculate from the data in Figure 2 that NH_4Cl treatment raised the pH sensed by intracellular HPTS to approximately 6.7–6.8. Figure 9 shows the similar effect of treatment with monensin, but the pH reported was slightly more acidic than achieved with 50 mM NH_4Cl.

Rapid reversal of alkalinization upon removal of NH_4Cl or monensin suggests the buffering capacity of intravesicular HPTS is not large compared to the ability of endocytic vesicles to reestablish a proton gradient.

Nature of the Liposome Binding Site and Rate of Liposome Clearance from the Cell Surface. As described above, the mean pH reported by liposome-encapsulated HPTS was approximately 7.1 following 15 min of liposome–cell interaction (Figure 8B). Such a value seemed high, given the more rapid acidification reported for a variety of ligands that enter cells by receptor-mediated endocytosis (Tycko & Maxfield, 1982; Murphy et al, 1984). As the observed value may be biased toward the alkaline by a preponderance of surface-bound liposomes, we undertook to determine the longevity the cell-surface pool. CV-1 cells were treated as described above, except that liposome–cell interaction was terminated by extensive washing in ice-cold buffer and cells were removed from the culture substrate by trypsin treatment in the cold. Cells in suspension were analyzed directly or washed free of eluted liposomes by centrifugation. The magnitude and the rate of change in the λ_{EX} 450/413 nm ratio obtained from suspended cells was similar to that for cells on coverslips: that is, a progressive reduction of the F_{EM} ratio with λ_{EX} 450/413 nm from nearly identical starting values and a progressive increase in the ratio with λ_{EX} 403/413 nm (data not shown). When trypsinized cells were compared to those that had been washed subsequently by centrifugation, it was observed that washed cells had a lower total associated fluorescence, as well as HPTS at a lower average pH. Control experiments showed that trypsin did not induce leakage of liposome contents (not shown). Thirty minutes after liposome addition, approximately 30% of the total fluorescence could be removed from the cells (not shown), and the pH reported was approximately 0.2–0.3 unit lower for trypsinized, washed cells. The F_{EM} ratios for suspended cells reported progressively acidic pH with time; in parallel, the difference decreased between unwashed cells and trypsinized, washed suspension cells. By 2.0 h, no difference was detected, either in F_{EM} ratio or in total cellular HPTS fluorescence (not shown). These results suggest that a portion of the cell-associated liposomes, most likely those on the cell surface, could be removed by incubation with mild trypsinization. With longer incubation time, that population of liposomes became resistant to elution. We infer that continuing endocytosis, in part via protease-sensitive cell-surface components, is the process leading to irreversible association of liposome contents with cells.

Intracellular Fate of HPTS-Containing Liposomes. HPTS in an acidic environment is highly fluorescent with excitation at the appropriate wavelengths. In contrast, fluorescein-based compounds have no efficient excitation bands at low pH; Ohkuma and Poole (1978) show approximately 85% reduction in peak fluorescein F_{EM} over the pH range 7.4–5.5. Thus fluorescence microscopy of fluorescein-loaded cells is biased toward visualization of compartments with high concentrations of dye and high pH and away from compartments with acidic pH or more dilute dye. HPTS reveals a progression of liposome contents to compartments not observed in previous studies using carboxyfluorescein and calcein (Straubinger et al., 1983). In the present work, we have observed living cells by video microscopy under low-light conditions and have discovered that some dynamic intracellular vesicles may be labeled with liposome-delivered HPTS.

For video microscopy, cells were exposed to 5-fold lower concentrations of liposomes (20 nmol) to promote more synchronous endocytosis and reduce total cell-associated fluorescence. Two striking features became apparent with continued observation of cells under low-light conditions. First, highly motile vesicles became labeled with HPTS, particularly in the cell periphery (not shown). Labeled vesicles were translated substantial distances (up to 20 μm) and with a substantial rate (2 μm/s). HPTS spectral properties revealed that such vesicles were acidic. However, the lack of suitable image-processing equipment precluded an estimation of the pH of individual vesicles. Thus, we could not determine whether a progression toward more acidic pH occurs in such vesicles.

A second striking observation was the labeling of tubular organelles with liposome-delivered material. Figure 10A shows such an organelle, under violet excitation (λ_{EX} 350–410 nm). Tubular structures frequently were observed 1–2 h after initial exposure of cells to HPTS liposomes. The structure shown here (Figure 10A) was a single tubule, although ramified

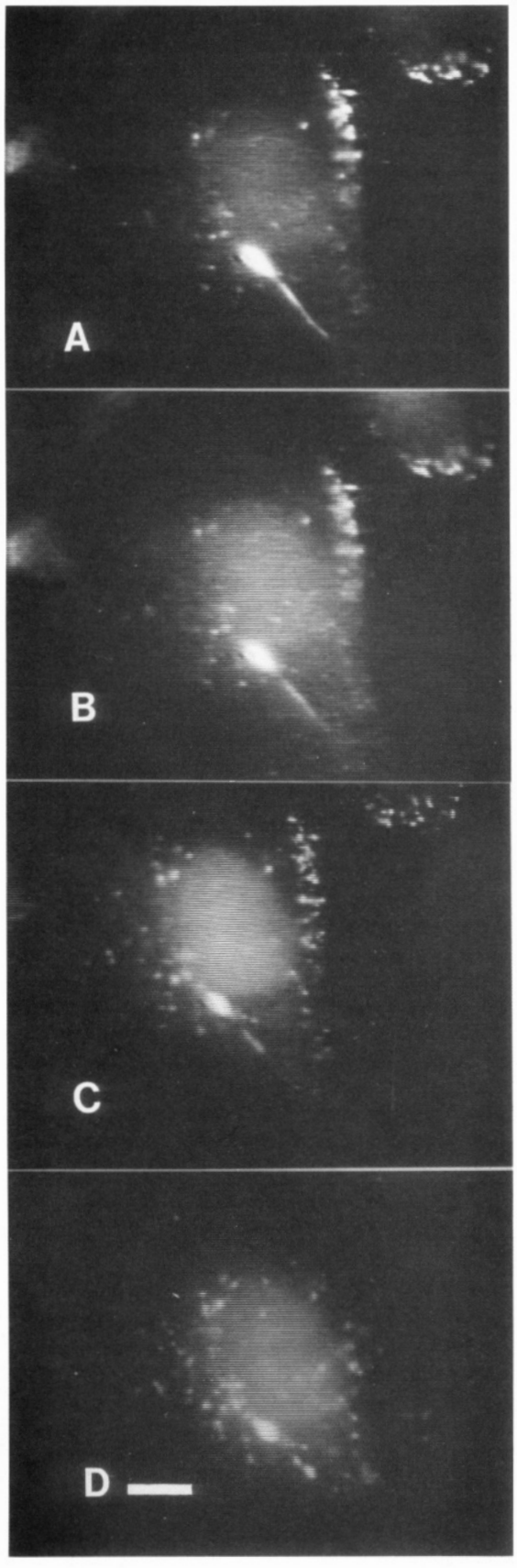

FIGURE 10: Dynamic rearrangement of tubular organelles labeled by liposome-delivered HPTS. Cell monolayers were exposed to 20 nmol of liposomes as in Figure 4 and observed 1.5 h after free liposomes were removed. Video intensification was used to observe cells continuously under low-light conditions (Materials and Methods). All frames show total cell-associated HPTS under violet band excitation ($\lambda_{EX\ VIOLET}$). Elapsed time for the entire series was approximately 2.5 min. (A) Time 0; (B) 60 s; (C) 100 s; (D) 145 s. Bar: 10 μm.

structures have been observed. Recently, organelles of similar morphology have received increased attention (Robinson et al., 1986; Swanson et al., 1987). Such structures were labeled previously by pinocytosis of the pH-insensitive dye Lucifer yellow and visualized by fluorescence microscopy, as well as by electron microscopy. Previously reported tubules are lysosomal, in that they contain acid phosphatase and cathepsin L (Robinson et al., 1986; Swanson et al., 1987). One would infer from the presence of such enzymes that these organelles have an acidic lumen.

From the pH-dependent spectral properties of HPTS, we have determined that the tubular organelles observed here are acidic. Illumination with violet wavelengths gave a total cell-associated fluorescence intensity close to that expected for 7 μM HPTS. HPTS fluorescence under blue illumination was below the sensitivity of the photometer. As noted above, pH 5.5–6 is the range in which the intensity of 7 μM dye is undetectable under $\lambda_{EX\ BLUE}$. At present it is not possible to assign a more accurate pH for the tubular organelles.

The tubular organelles observed were dynamic structures. Figure 10 shows a sequence of images taken over a period <150 s. During 50 s subsequent to Figure 10A, constrictions formed in the tubule (Figure 10B). The constriction progressed to separation of the organelle into two entities over 40 (Figure 10, frames C and D). One of the products was nonmotile, a large punctate of approximately 2–4-μm diameter; the other remained tubular during subsequent observation. Variation in the shape of the organelle with time (Figure 10) suggests that association with a force-generating substrate may be responsible for the observed tubular shape. Release of tension following fission would explain relaxation of daughter structures into rounder vesicles. Swanson et al. (1987) have shown that tubular lysosome morphology is dependent on microtubule integrity, as well as proximity of those entities.

Previously, Robinson et al. (1986) noted fragmentation of tubular lysosomes during observation under fluorescence illumination and suggested that the fragmentation could be an artifact produced by prolonged irradiation. Our observations under light levels lower than those present in conventional fluorescence microscopy suggest that the dynamic nature of the organelle may not be an artifact. Furthermore, intracellular organelles remained motile during observation; it has been noted previously that some classes of motile organelles halt as a result of photodamage [cf. Pastan and Willingham (1981)].

Discussion

A variety of molecules are endocytosed by cells and enter through a coated pit/coated vesicle pathway. The fate of endocytosed molecules can vary from rapid recycling to the cell surface to progression through a variety of intracellular compartments (Brown & Goldstein, 1979; Steinman et al., 1983; Mellman et al., 1986). By comparison, our understanding of the mechanism and pathway for liposome endocytosis and processing still is very restricted. The nature of the signals and receptors mediating endocytosis of liposomes is unknown and may not consist of a single molecular entity. Therefore, classical receptor biochemistry has been difficult. Reversibility of liposome–cell binding may be incomplete, except in cases where ligands such as antibodies are wholly responsible for the binding interaction. As a result, it has been difficult to discriminate between surface-bound and endocytosed liposomes and therefore difficult to determine the kinetics of liposome internalization.

We have described a new method for kinetic analysis of endocytosis in living cells and have applied it to tracking the

intracellular distribution of liposome contents. In our approach, 8-hydroxy-1,3,6-pyrenetrisulfonate, a membrane-impermeant, pH-sensitive fluorescent compound, is entrapped within the aqueous compartment of liposomes. Endocytosis is detected by the large shift in excitation wavelength that HPTS undergoes upon acidification. As a suitable fluorescence indicator, HPTS provides several advantages: a pK_a value in the physiological range, a high fluorescence quantum yield, a fluorescence emission maximum (510 nm) well above 450 nm, which minimizes interference due to background emission of biological fluids, and good water solubility and photostability (Wolfbeis et al., 1983). With fluorescence microscope optics commonly available, dye in acidic compartments can be distinguished readily from dye in a neutral environment. HPTS fluorescence is most sensitive in the pH range 5–7 and is ideally suited for studies on the early events of endocytosis. The dye has been encapsulated previously to measure proton permeation of bilayer membranes (Biegel & Gould, 1981; Clement & Gould, 1981) and to measure cytoplasmic pH in fibroblasts (Giuliano & Gillies, 1987). In the present study, fluorometry has been used as a qualitative measure of the rate and extent of liposome acidification within populations of cells. Fluorescence microscopy has been used to gain a qualitative view of the variability of endocytosis among individually observed cells and has revealed asynchronous internalization of individual liposomes in single cells.

The pinocytic loading of cells with free HPTS, allbeit less efficient than loading by means of liposomes, is itself significant. While such experiments were undertaken here as controls to estimate the contribution of leaked dye to our observations on liposome endocytosis, free HPTS as a marker of fluid-phase pinocytosis may have advantages over fluorescein-based dyes such as FTC–dextran (Ohkuma & Poole, 1978) and carboxyfluorescein [cf. Goldmacher et al. (1986)]. The more distinct pH-dependent excitation shift and stable isosbestic point of HPTS may allow measurements of intravesicular pH with greater accuracy or less correction than possible with other markers. The fact that HPTS reports pH as well as internalization may provide additional information on early events in pinocytosis. Pinocytosis of free HPTS at 350 μM was clearly detectable after 30 min. Longer incubations or higher concentrations of HPTS, comparable to those used in loading cells (Robinson et al., 1986) with such markers as Lucifer yellow (Stewart, 1978), should give high, uniform labeling. Future studies will examine the acceptability of HPTS for such purposes.

The view of liposome–cell interactions afforded by HPTS, as revealed in the experiments described here, contrasts sharply with our earlier appreciation of the intracellular fate of liposomes. In a previous study that employed fluorescence and electron microscopy to study liposome fate (Straubinger et al., 1983), we obtained a static picture of the long-term fate of liposomes and their contents. Colloidal gold encapsulated in liposomes accumulated with time in electron-dense bodies we inferred to be lysosomes. Fluorescein-based probes showed perinuclear accumulations of fluorescence. Neither technique revealed the variety of organelles contacted by liposome contents nor the dynamic nature of the those organelles.

The rate and maximal acidification of liposome contents to pH 5.6 (seen at 3–24 h) contrast with results obtained from different cells by use of other probes. DeDuve (1974) and Ohkuma and Poole (1978) used independent methods to determine the mean pH of a compartment in macrophages considered lysosomal; their values were in the pH range 4.6–4.8. Our results suggest a minimum average pH greater than 5.5 for liposome contents in CV-1 cells. Such a value is comparable to those determined in fibroblasts subsequent to receptor-mediated endocytosis [cf. Maxfield (1982) and Murphy et al. (1984)]. However, the rate at which liposome-delivered HPTS approaches that pH apparently is slower than that demonstrated for probes that enter cells by receptor-mediated endocytosis (Tycko & Maxfield, 1982; Murphy et al., 1984). We conclude that liposomes may have an intracellular fate that is only partly similar to that of markers for receptor-mediated endocytosis. Although the process mediating the adhesion of liposomes to the cell surface is as yet unknown, surface binding leads to endocytosis in coated pits (Straubinger et al., 1983). It is possible that liposomes bind to slowly internalized cell-surface structures, pass more slowly through the various intracellular vesicle sorting points subsequent to endocytosis, or that liposome contents passively label compartments of several intracellular paths, including the recycling pathway. If the latter were to occur, it would be possible that the average pH reported by cell-associated HPTS would fall relatively slowly as dye in more alkaline recycling compartments was regurgitated. HPTS remaining within cells likely would reside in a nonrecycling compartment (Goldmacher et al., 1986) which could have a lower mean pH.

Elucidation of the characteristics of liposome endocytosis is important to the application of liposomes as probes of endocytic function (Chin et al., 1989) and as carriers, either for intracellular delivery of macromolecules or from modifying distribution of encapsulated drugs in vivo. In the former application, liposomes containing HPTS may be used as probes of coated-pit-dependent endocytosis, as an aid in dissecting the molecular controls of that process. In the present study, liposomes contained approximately 5×10^4 fluorescent reporter molecules. Thus, endocytosis of a single liposome can be detected with appropriate optics and microscope. In contrast, common ligands such as transferrin may bear as few as two to four fluorescent reporter molecules per molecule, thus reducing the sensitivity of such a method for detecting endocytosis.

In the latter application, endocytosis is a major parameter in determining the efficiency of cytoplasmic delivery or the rate of clearance of liposomes from the circulation. Insight into the intracellular pathway has given rise to a new class of liposomes for intracellular delivery. In an attempt to mimic viruses that use pH as a specific trigger to transfer their nucleocapsid to the cytoplasm (White et al., 1983), the known physical properties of specific phospholipids and fatty acids have been exploited to produce pH-sensitive liposomes (Connor & Huang, 1985; Düzgünes et al., 1985; Straubinger et al., 1985) that undergo major structural changes in a mildly acidic environment (pH 6.3–6.8). Other strategies to produce pH-sensitive membranes with pure-lipid systems also have been successful (Yatvin et al., 1980; Connor et al., 1984; Ellens et al., 1985; Nayar & Shroit, 1985). pH-sensitive liposomes have been shown to deliver large and impermeant molecules such as fluorescent dextran, toxins, and DNA to the cytoplasm (Straubinger et al., 1985; Collins & Huang, 1987). While fusion of pH-sensitive liposomes with the endosome membrane is an attractive hypothesis, the mechanism of cytoplasmic delivery is largely unknown.

An understanding of liposome–cell interaction and the intracellular pathway already has had an impact on the use of liposomes as vehicles for intracellular delivery. For example, delivery of methotrexate γ-aspartate and 5-fluoroorotate (Heath et al., 1983, 1985), transport-negative analogues of currently used cancer chemotherapeutic agents, has provided

highly specific toxicity to the cells to which ligand-bearing liposomes (Machy et al., 1982; Huang et al., 1983; Heath et al., 1983, 1985) have been targeted. Inefficient endocytosis of some cell-surface antigens is a major factor that may, in some cases, reduce the effectiveness of such an approach (Straubinger et al., 1988). The method described here will allow rapid screening for ligands that, when covalently bound to the liposome surface, mediate efficient endocytosis.

Added in Proof

Daleke et al. (1990) have applied this method for a detailed analysis of liposome endocytosis by macrophages.

Acknowledgments

We thank Dr. E. Schulze for providing access to video image processing equipment of the Department of Biochemistry (UCSF) and for the benefit of his expertise in performing those experiments.

Registry No. Pyranine, 6358-69-6.

References

Barbet, J., Machy, P., Truneh, A., & Leserman, L. D. (1984) Weak-acid induced release of liposome-encapsulated carboxyfluorescein, *Biochim. Biophys. Acta 772*, 347–56.

Bartlett, G. R. (1959) Phosphorus assay in column chromatography, *J. Biol. Chem. 234*, 466–8.

Biegel, C. M., & Gould, J. M. (1981) Kinetics of hydrogen ion diffusion across phospholipid vesicle membranes, *Biochemistry 20*, 3474–9.

Brown, M. S., & Goldstein, J. L. (1979) Receptor-mediated endocytosis: insights from the lipoprotein receptor system, *Proc. Natl. Acad. Sci. U.S.A. 75*, 3330–7.

Brown, M. S., Anderson, R. G. W., & Goldstein, J. L. (1983) Recycling receptors: the round-trip itinerary of migrant membrane proteins, *Cell 32*, 663–7.

Chin, D. J., Straubinger, R. M., Acton, S. Näthke, I., & Brodsky, F. M. (1989) 100-kD polypeptides in peripheral clathrin-coated vesicles are required for receptor-mediated endocytosis, *Proc. Natl. Acad. Sci. U.S.A. 86*, 9289–93.

Clement, N. R., & Gould, J. M. (1981) Pyranine (8-hydroxy-1,3,6-pyrenetrisulfonate) as a probe of internal aqueous hydrogen ion concentration in phospholipid vesicles, *Biochemistry 20*, 1534–8.

Collins, D., & Huang, L. (1987) Cytotoxicity of diphtheria toxin A fragment to toxin-resistant murine cells delivered by pH-sensitive immunoliposomes, *Cancer Res. 47*, 735–9.

Connor, J., & Huang, L. (1985) Efficient cytoplasmic delivery of a fluorescent dye by pH-sensitive immunoliposomes, *J. Cell Biol. 101*, 582–9.

Connor, J., & Huang, L. (1986) pH-sensitive immunoliposomes as an efficient and target-specific carrier for antitumor drugs, *Cancer Res. 46*, 3431–5.

Connor, J., Yatvin, M. B., & Huang, L. (1984) pH-sensitive liposomes: acid-induced liposome fusion, *Proc. Natl. Acad. Sci. U.S.A. 81*, 1715–8.

Daleke, D., Hong, K., & Papahadjopoulos, D. (1990) *Biochim. Biophys. Acta* (in press).

DeDuve, C., DeBarsy, T., Poole, B., Trouet, A., Tulkens, P., & VanHoof, F. (1974) Lysosomotropic agents, *Biochem. Pharmacol. 23*, 2495–2531.

Düzgünes, N., Straubinger, R. M., Baldwin, P. A., Friend, D. S., & Papahadjopoulos, D. (1985) Proton-induced fusion of oleic acid–phosphatidylethanolamine liposomes, *Biochemistry 24*, 3091–8.

Ellens, H., Bentz, J., & Szoka, F. C. (1985) H^+- and Ca^{2+}-induced fusion and destabilization of liposomes, *Biochemistry 24*, 3099–106.

Fraley, R., Straubinger, R. M., Rule, G., Springer, E. L., & Papahadjopoulos, D. (1981) Liposome-mediated delivery of DNA to cells: enhanced efficiency of delivery by changes in lipid composition and incubation conditions, *Biochemistry 20*, 6978–87.

Gardas, A., & Macpherson, I. (1979) Microinjection of ricin entrapped in unilamellar liposomes into a ricin-resistant mutant of baby hamster kidney cells, *Biochim. Biophys. Acta 584*, 538–41.

Giuliano, K. A., & Gillies, R. J. (1987) Determination of intracellular pH of BALB/c-3T3 cells using the fluorescence of pyranine, *Anal. Biochem. 167*, 362–71.

Goldmacher, V. S., Tinnel, N. L., & Nelson, B. C. (1986) Evidence that pinocytosis in lymphoid cells has low capacity, *J. Cell Biol. 102*, 1312–9.

Haylett, T., & Thilo, L. (1986) Limited and selective transfer of plasma membrane glycoproteins to membrane of secondary lysosomes, *J. Cell Biol. 103*, 1249–56.

Heath, T. D., Montgomery, J. A., Piper, J. R., & Papahadjopoulos, D. (1983) Antibody-targeted liposomes: increase in specific toxicity of methotrexate-γ-aspartate, *Proc. Natl. Acad. Sci. U.S.A. 80*, 1377–81.

Heath, T. D., Lopez, N. G., Stern, W. H., & Papahadjopoulos, D. (1985) 5-Fluoro orotate: a new liposome-dependent cytotoxic agent, *FEBS Lett. 187*, 73–5.

Hong, K., Straubinger, R. M., & Papahadjopoulos, D. (1986) Fluorometric analysis of liposome-dependent endocytosis, *J. Cell Biol. 103*, 569a.

Hong, K., Düzgünes, N., Meers, P. R., & Papahadjopoulos, D. (1987) Protein modulation of membrane fusion, in *Cell Fusion* (Sowers, A. E., Ed.) pp 269–84, Plenum Press, New York.

Huang, A., Kennel, S. J., & Huang, L. (1983) Interactions of immunoliposomes with target cells, *J. Biol. Chem. 258*, 14034–40.

Klappe, K., Wilschut, J., Nir, S., & Hoekstra, D. (1986) Parameters affecting fusion between Sendai virus and liposomes. Role of viral proteins, liposome composition, and pH, *Biochemistry 25*, 8252–60.

Lopez-Berestein, G., Fainstein, V., Hopfer, R., Mehta, K., Sullivan, M. P., Keating, M., Rosenblum, M. G., Mehta, R., Luna, M., Hersh, E. M., Reuben, J., Juliano, R. L., & Bodey, G. P. (1985) Liposomal amphotericin B for the treatment of systemic fungal infections in humans: a preliminary study, *J. Infect. Dis. 151*, 704–10.

Machy, P., Barbet, J., & Leserman, L. D. (1982) Differential endocytosis of T and B lymphocyte surface molecules evaluated with antibody-bearing fluorescent liposomes containing methotrexate, *Proc. Natl. Acad. Sci. U.S.A. 79*, 4148–52.

Maxfield, F. R. (1982) Weak bases and ionophores rapidly and reversibly raise the pH of endocytic vesicles in cultured mouse fibroblasts, *J. Cell Biol. 95*, 676–81.

Mayhew, E., & Papahadjopoulos, D. (1983) Therapeutic applications of liposomes, in *Liposomes* (Ostro, M., Ed.) pp 289–341, Marcel Dekker, New York.

Mayhew, E., Rustum, Y., & Vale, W. J. (1984) Inhibition of liver metastases of M5076 tumor by liposome-entrapped adriamycin, *Cancer Drug Delivery 1*, 43–58.

McIntosh, D. P., & Heath, T. D. (1982) Liposome-mediated delivery of ribosome-inactivating proteins to cells in vitro, *Biochim. Biophys. Acta 690*, 224–30.

Meers, P., Ernst, J. D., Hong, K., Fedor, J., Goldstein, I. M., & Papahadjopoulos, D. (1987) Synexin-like proteins in the cytosol of polymorphonuclear leukocytes: identification and characterization of granule-aggregating and membrane-fusing activities, *J. Biol. Chem. 262*, 7950–8.

Mellman, I., Fuchs, R., & Helenius, A. (1986) Acidification of the endocytic and exocytic pathways, *Annu. Rev. Biochem. 55*, 663–700.

Murphy, R. F., Powers, S., & Cantor, C. R. (1984) Endosomal pH measured in single cells by dual fluorescence flow cytometry: rapid acidification of insulin to pH 6, *J. Cell Biol. 98*, 1757–62.

Nayar, R., & Shroit, A. J. (1985) Generation of pH-sensitive liposomes: use of large unilamellar vesicles containing N-succinyldioleoylphosphatidylethanolamine, *Biochemistry 24*, 5967–71.

Nir, S., Klappe, K., & Hoekstra, D. (1986) Kinetics and extent of fusion between Sendai virus and erythrocyte ghosts: application of a mass action kinetic model, *Biochemistry 25*, 2155–61.

Ohkuma, S., & Poole, B. (1978) Fluorescence probe measurement of the intralysosomal pH in living cells and the perturbation of pH by various agents, *Proc. Natl. Acad. Sci. U.S.A. 79*, 2578–62.

Pastan, I. H., & Willingham, M. C. (1981) Journey to the center of the cell: role of the receptosome, *Science 214*, 504–9.

Reisine, T., Rougon, G., & Barbet, J. (1986) Liposome delivery of cyclic AMP-dependent protein kinase inhibitor into intact cells: specific blockade of cyclic AMP-mediated adrenocorticotropin release from mouse anterior pituitary tumor cells, *J. Cell Biol. 102*, 1630–7.

Robinson, J. M., Okada, T., Castellot, J. J., Jr., & Karnovsky, M. J. (1986) Unusual lysosomes in aortic smooth muscle cells: presence in living and rapidly-frozen cells, *J. Cell Biol. 102*, 1615–22.

Steinman, R. M., Mellman, I. S., Muller, W. A., & Cohn, Z. A. (1983) Endocytosis and the recycling of plasma membrane, *J. Cell Biol. 96*, 1–27.

Stewart, W. W. (1978) Functional connections between cells as revealed by dye-coupling with a highly fluorescent naphthalamide tracer, *Cell 14*, 741–59.

Straubinger, R. M., Hong, K., Friend, D. S., & Papahadjopoulos, D. (1983) Endocytosis of liposomes and intracellular fate of encapsulated contents: encounter with a low-pH compartment after internalization in coated vesicles, *Cell 32*, 1069–79.

Straubinger, R. M., Düzgünes, N., & Papahadjopoulos, D. (1985) pH-sensitive liposomes mediate cytoplasmic delivery of encapsulated macromolecules, *FEBS Lett. 179*, 148–54.

Straubinger, R. M., Lopez, N. G., Debs, R. J., Hong, K., & Papahadjopoulos, D. (1988) Liposome-based therapy of human ovarian cancer: liposome-cell interaction controls potency of negatively-charged and antibody-targeted liposomes, *Cancer Res. 48*, 5237–45.

Swanson, J., Bushnell, A., & Silverstein, S. C. (1987) Tubular lysosome morphology and distribution within macrophages depend on the integrity of cytoplasmic microtubules, *Proc. Natl. Acad. Sci. U.S.A. 84*, 1921–5.

Szoka, F. C., & Papahadjopoulos, D. (1978) Procedure for preparation of liposomes with large internal aqueous space and high capture by reverse-phase evaporation, *Proc. Natl. Acad. Sci. U.S.A. 75*, 4194–8.

Szoka, F. C., Jacobson, K., & Papahadjopoulos, D. (1979) The use of aqueous space markers to determine the mechanism of liposome-cell interaction, *Biochim. Biophys. Acta 551*, 295–303.

Szoka, F. C., Olson, F., Heath, T., Vail, W., Mayhew, E., & Papahadjopoulos, D. (1980) Preparation of unilamellar liposomes of intermediate size (0.1–0.2 μm) by a combination of reverse phase evaporation and extrusion through polycarbonate membranes, *Biochim. Biophys. Acta 601*, 559–71.

Tartakoff, A. M., (1983) Perturbation of vesicular traffic with the carboxylic ionophore monensin, *Cell 32*, 1026–8.

Truneh, A., Mishal, Z., Barbet, J., Machy, P., & Leserman, L. D. (1983) Endocytosis of liposomes bound to cell surface proteins measured by flow cytofluorometry, *Biochem. J. 214*, 189–94.

Tycko, B., & Maxfield, F. R. (1982) Rapid acidification of endocytic vesicles containing α_2-macroglobulin, *Cell 26*, 643–51.

White, J. M., & Helenius, A. (1980) pH-dependent fusion between the Semliki Forest virus membrane and liposomes, *Proc. Natl. Acad. Sci. U.S.A. 77*, 3273–7.

White, J. M., Kartenbeck, J., & Helenius, A. (1982) Membrane fusion activity of influenza virus, *EMBO J. 1*, 217–22.

White, J. M., Kielian, M., & Helenius, A. (1983) Membrane fusion proteins of enveloped animal viruses, *Q. Rev. Biophys. 16*, 151–95.

Wilson, T., Papahadjopoulos, D., & Taber, R. (1979) The introduction of poliovirus RNA into cells via lipid vesicles (liposomes), *Cell 17*, 77–84.

Wolfbeis, O. S., Fürlinger, E., Kroneis, H., & Marsoner, H. (1983) Fluorometric analysis. 1. A study on fluorescent indicators for measuring near neutral ("physiological") pH, *Fresenius' Z. Anal. Chem. 314*, 119–24.

Yatvin, M. B., Kreutz, W., Horwitz, B. A., & Shinitzky, M. (1980) pH-sensitive liposomes: possible clinical implications, *Science 210*, 1253–5.